Effects of Dispersion in Carbon Monoxide Adsorption and Carbon Monoxide Hydrogenation over Alumina-supported Ruthenium Catalysts

Toshio Okuhara,* Tomoo Kimura, Kenji Kobayashi,† Makoto Misono, and Yukio Yoneda
Department of Synthetic Chemistry, Faculty of Engineering, The University of Tokyo, Hongo, Bunkyo-ku, Tokyo 113

(Received July 23, 1983)

Ru/Al_2O_3 catalysts prepared from $[Ru_3(CO)_{12}]$ and from $RuCl_3$ were characterized by chemisorption of H_2 and CO, and by infrared measurement of adsorbed CO. By using these catalysts, the effect of the dispersion on the activity and selectivity in CO hydrogenation was studied. Ru/Al_2O_3 catalysts prepared from $[Ru_3(CO)_{12}]$ showed high dispersions (>80%), and were more active and selective for the production of olefins in the CO hydrogenation than Ru/Al_2O_3 catalysts prepared from $RuCl_3$. However, the distribution of product hydrocarbons was not sensitive to the Ru dispersion. Infrared study of adsorbed CO revealed that twin-type CO ($Ru(CO)_2$) as well as linear-type CO (Ru-CO) was present on each Ru/Al_2O_3. The twin-type CO was more strongly held and was less reactive to hydrogenation. For each series of Ru/Al_2O_3, the turnover frequency increased as the dispersion decreased. This change has been explained by the poisoning effect of the twin-type CO. The higher activity of Ru/Al_2O_3(A) was ascribed to the lower concentration of the twin-type CO on the surface.

In Fisher-Tropsh synthesis, Ru shows high activity and selectivity for the production of long-chain hydrocarbons.[1] The effect of Ru dispersion on the activity of this reaction has been studied by several workers.[2–6] King reported that the turnover frequency (abbreviated as TOF) of both methane formation and CO conversion over supported Ru catalysts declined as the dispersion increased.[2] This is in contrast with the case of Pt or Pd.[7] Kikuchi *et al.* also observed similar changes of TOF with the dispersion over Ru/Al_2O_3 and Ru/V_2O_3. However, TOF over Ru/V_2O_3 was considerably higher than that over Ru/Al_2O_3, indicating that the TOF was dependent not only on the dispersion but also on the nature of the supports.[5] Fujimoto *et al.* reported that the change of TOF with Ru dispersion appeared in a different manner depending on the reaction conditions.[6]

The dispersions of Ru catalysts used in the above studies were limited up to 60%. The authors[8] and Bell *et al.*[4,9] found that Ru/Al_2O_3 prepared from carbonyl complex like $[Ru_3(CO)_{12}]$ or $[Ru_6C(CO)_{17}]$ showed dispersions higher than 60%. As for the highly dispersed Ru/Al_2O_3, Kellner and Bell[4] reported that the TOF decreased as the dispersion increased up to 90%. On the other hand, the authors observed that the TOF for the Ru/Al_2O_3 prepared from $[Ru_3(CO)_{12}]$ was unexpectedly high at high Ru loading levels.[10]

Recently, infrared spectroscopic studies[11–14] have shed light on the surface state of Ru catalysts under reaction conditions. The Ru surface was almost entirely covered by adsorbed CO during the hydrogenation of CO,[11] and the active sites were limited to a small portion of the metal surface.[12] Kellner and Bell,[4,9] and the authors[15] showed that both linear-type CO and twin-type CO (diadsorbed CO) were present on Ru/Al_2O_3. However, there are very few instances in which physical properties and catalysis of highly dispersed Ru catalysts were studied concurrently.

The present study was undertaken to determine the prime factor controlling the change of the TOF with the dispersion of Ru, since, in spite of several efforts, the reason why TOF changes with dispersion has not yet been clarified. The Ru/Al_2O_3 catalysts having a wide range of dispersion were systematically prepared from $RuCl_3$ and $[Ru_3(CO)_{12}]$. By the use of these catalysts, the influences of preparation method and dispersion on the TOF, product distribution and olefin/paraffin ratio were investigated. Moreover, infrared measurement of adsorbed CO was performed to elucidate the strength of adsorption, the reactivity toward hydrogenation and the role of each adsorbed CO in the catalytic reaction.

Experimental

Catalysts. Ru/Al_2O_3 catalysts were prepared using γ-Al_2O_3 (Reference Catalyst of the Catalysis Society of Japan, ALO-4, 170 $m^2\,g^{-1}$) from $[Ru_3(CO)_{12}]$ (Strem Chemical Co.) and $RuCl_3\cdot 3H_2O$ (Kanto Chemical). $[Ru_3(CO)_{12}]$ was adsorbed from hexane solution at room temperature onto the Al_2O_3 which had been dried in a N_2 flow at 450 °C. Then the solvent was removed in a stream of N_2 at room temperature. The catalysts obtained by the decomposition and reduction with H_2 at 450 °C are designated as Ru/Al_2O_3 (A) hereafter. The second class of Ru/Al_2O_3 catalysts were prepared by incipient wetness impregnation with an aqueous solution of $RuCl_3$ and are designated as Ru/Al_2O_3 (B). The loading amount of Ru metal was altered from 0.9 to 4% for Ru/Al_2O_3 (A) and 0.5 to 5% for Ru/Al_2O_3 (B).

Chemisorption of hydrogen and CO. The pretreatment conditions and procedure have been described in the previous paper.[15] Chemisorption measurement was carried out at room temperature in a conventional static system having a volume of 60 cm^3. Since adsorption of hydrogen to Al_2O_3 alone was negligible, the dispersion of Ru was calculated from the total uptake of hydrogen under an equilibrium pressure of about 60 mmHg. The chemisorption of CO on Ru was calculated from the differences in the uptake of CO between Ru/Al_2O_3 and Al_2O_3 under an equilibrium pressure of about 40 mmHg.

Catalytic Reactions. After the evacuation of the catalyst at 450 °C for 1 h, the catalyst was reduced with H_2 (600 mmHg (1 mmHg≈133.322 Pa)) at 450 °C for 2 h in a closed circulation system having a volume of about 200 cm^3. Then the catalyst was cooled *in vacuo* to 200 °C. Hydrogenation of CO was carried out at 200 °C under the total pressure of about 500 mmHg ($H_2/CO=2$) in the same system. The reaction was repeated by replacing the reactant gases after a short period of evacuation (≃10 min). The rate and the

---

† Present address: Nippon Electric Co., Ltd.

distribution of product hydrocarbons were determined at about 10—30% conversion in the second run, in which the reaction proceeded at a steady rate and the selectivity was independent of the conversion in the above conversion range. The product hydrocarbons except for methane were collected in a trap kept at liquid-nitrogen temperature during the reaction to prevent the secondary reactions such as hydrogenation of olefins and hydrogenolysis of products. Actually, when the reaction was carried out without a liquid-nitrogen trap, considerable increases of both methane and paraffin fractions were observed. The column materials used for gas chromatographic analyses consisted of Molecular Sieve 5A (25 °C) to separate methane and CO, and Porapak Q (60 °C) to separate CO_2, ethylene and ethane. A VZ-7 column (kept at 25 °C) was used for C_3 through C_6 hydrocarbons. The formation of methanol and ethanol was checked with Porapak Q (100 °C), but was not detected. Hydrogenolysis of ethane was also carried out at 150 °C in the same system under the initial pressure of 108 mmHg (H_2/ethane=2) after the same pretreatment as in the case of the hydrogenation of CO.

Infrared Spectroscopy. The procedure has been described in the previous paper.[15] The catalyst was first kept in contact with CO (20 mmHg) at room temperature for 0.5 h. After CO was evacuated at desired temperatures for 1 h, infrared spectra were recorded using a Fourier-transform spectrometer (JEOL JIR 10) at room temperature. The weight of the sample disk was about 60 mg for all catalysts.

Results

Chemisorption of Hydrogen and CO. H/Ru and CO/Ru are summarized in Table 1, where the H/Ru or CO/Ru=number of hydrogen atoms or CO molecules chemisorbed/number of Ru in the catalysts. In the chemisorption of hydrogen, the H/Ru ratio was higher than 0.79 for all Ru/Al_2O_3 (A). The H/Ru for Ru/Al_2O_3 (B) progressively increased as Ru concentration decreased, but they were not more than 0.41. Hereafter, the dispersion of the Ru will be defined as H/Ru×100(%).

The CO/Ru ratio was always greater than the H/Ru. Particularly, in the case of low loading catalysts, *e.g.*, 0.5% Ru/Al_2O_3 (B) and 0.9% Ru/Al_2O_3 (A), high CO/Ru ratios (>1.4) were observed. The CO/H ratio reached 3.6 and 2.7 over 0.5 and 0.9% Ru/Al_2O_3 (B), respectively. The uptakes of H_2 and CO became very small (H/Ru=0.1, CO/Ru=0.1), when 2.5% Ru/Al_2O_3 (A) was pretreated with O_2 (50 mmHg) at 450 °C for 4 h followed by reduction with H_2 (600 mmHg) at 450 °C for 3 h.

TABLE 1. CHEMISORPTION OF H_2 AND CO ON RUTHENIUM CATALYSTS

Catalyst	wt%	H/Ru	CO/Ru	CO/H	$\bar{d}$/Å[a]
Ru/Al_2O_3(A)	0.9	0.85	1.41	1.7	(10)
(from[$Ru_3(CO)_{12}$])	2.5	0.82	1.10	1.3	(10)
	4.0	0.79	1.01	1.3	(11)
	2.5[b]	0.10	0.11	1.1	83
Ru/Al_2O_3(B)	0.5	0.41	1.46	3.6	20
(from $RuCl_3$)	0.9	0.38	1.03	2.7	22
	2.5	0.21	0.32	1.5	40
	5.0	0.18	0.26	1.4	46

a) Mean diameter calculated from the adsorption of hydrogen. b) Pre-oxidized sample.

The average particle size was calculated from the hydrogen adsorption as given in Table 1, by assuming that a hydrogen atom is adsorbed on an Ru atom at 1 : 1 stoichiometry and that the average area of Ru is 8.17 Å^2.[16] The average size of Ru particle on Ru/Al_2O_3 (B) was in the range of 20 to 46 Å, and was less than 10 Å for Ru/Al_2O_3 (A).

Activity and Selectivity. The rates of the CO hydrogenation per gram of Ru are plotted as a function of Ru loading in Fig. 1. The rate for Ru/Al_2O_3 (B) was much less susceptible to the Ru loading levels than that for Ru/Al_2O_3 (A). 4% Ru/Al_2O_3 (A), which was about 30 times more active than 0.9% Ru/Al_2O_3 (A), exhibited the highest activity among the Ru/Al_2O_3 catalysts used.

Figure 2 shows the olefin/paraffin ratio in C_2 through C_4 hydrocarbons as a function of the Ru dispersion. The ratios in these hydrocarbons increased monotonically as the dispersion increased. The selectivity to C_2–C_4 olefins among total hydrocarbons increased from about 40 to 60% in the range of the dispersion from 20 to 85%.

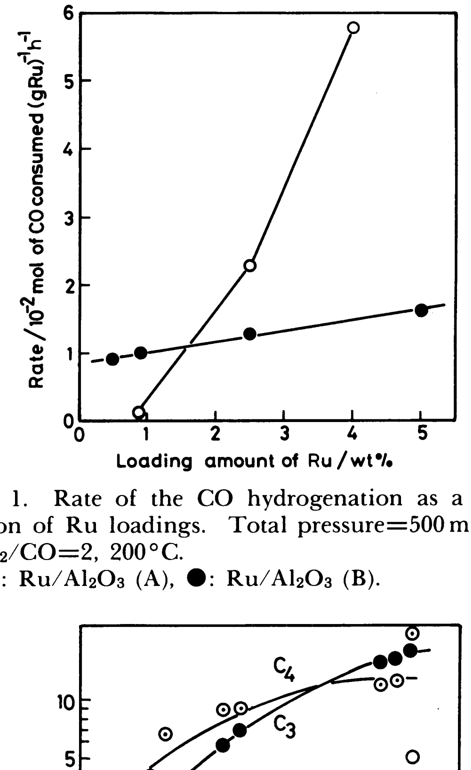

Fig. 1. Rate of the CO hydrogenation as a function of Ru loadings. Total pressure=500 mmHg, H_2/CO=2, 200 °C.
○: Ru/Al_2O_3 (A), ●: Ru/Al_2O_3 (B).

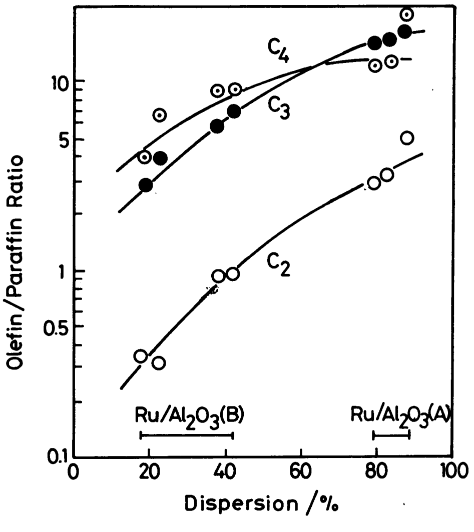

Fig. 2. Effect of Ru dispersion on olefin/paraffin ratio in the CO hydrogenation.

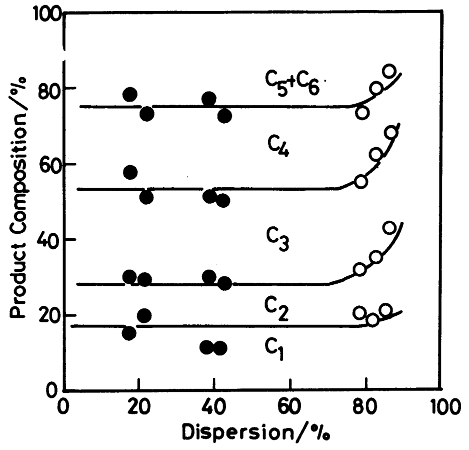

Fig. 3. Effect of Ru dispersion on product composition in the CO hydrogenation.

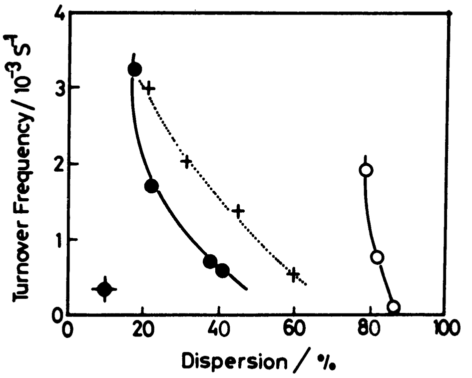

Fig. 4. Change of turnover frequency for the CO hydrogenation as a function of Ru dispersion at 200 °C.

○: Ru/Al_2O_3 (A), ●: Ru/Al_2O_3 (B), ◆: Pre-oxidized 2.5% Ru/Al_2O_3 (A), +: King's data.

The influences of the dispersion on the product distribution are shown in Fig. 3. Except for a slight increase in the fraction of C_2 through C_4 hydrocarbons at very high dispersions, the distribution of product hydrocarbons was nearly constant over the wide range of dispersion. The preoxidized 2.5% Ru/Al_2O_3 (A) exhibited an unusual activity and selectivity. The activity for the CO hydrogenation was 1/16 of 2.5% Ru/Al_2O_3 (A) treated ordinarily and methane was the main product ($\simeq$70%).

In Fig. 4, the TOF for CO hydrogenation was plotted as a function of the Ru dispersion. King's data for Ru/Al_2O_3,[2] which were adjusted to the present reaction conditions, assuming that the pressure dependence and activation energy were the same as those reported by Vannice,[17] are also shown in Fig. 4. The TOF-dispersion correlation showed two separate lines in Fig. 4. The TOF obtained over Ru/Al_2O_3 (B) is consistent with King's data. On the other hand, with the exception of the dispersion of 85%, the TOF of Ru/Al_2O_3 (A) was appreciably higher than that expected from Ru/Al_2O_3 (B). It is noted that the TOF for the pre-oxidized 2.5% Ru/Al_2O_3 (A) is far below the two lines. In contrast with the CO hydrogenation, the TOF for the hydrogenolysis of ethane was nearly constant, except for 0.9% Ru/Al_2O_3 (A), as shown in Fig. 5.

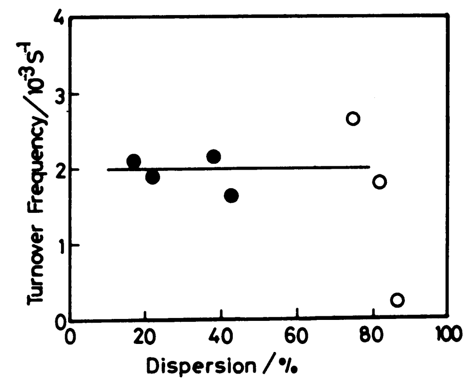

Fig. 5. Change of turnover frequency for the hydrogenolysis of ethane as a function of Ru dispersion at 150 °C.

○: Ru/Al_2O_3 (A), ●: Ru/Al_2O_3 (B).

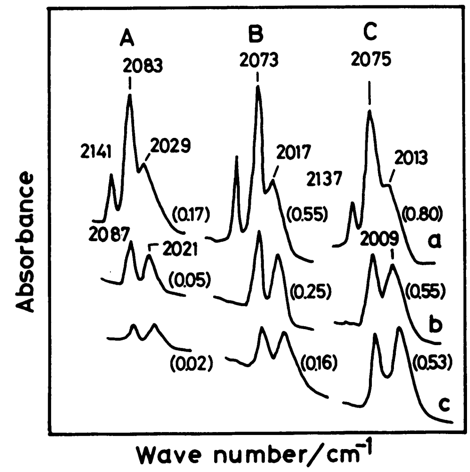

Fig. 6. Changes of infrared spectra of CO adsorbed on Ru/Al_2O_3 (B) by evacuation or hydrogenation: (A) 5 wt%, (B) 2.5 wt%, (C) 0.5 wt%; (a) after evacuation at 25 °C, (b) after evacuation at 200 °C, (c) after the reaction with H_2 (100 mmHg) at 200 °C for 1 h. Figures in parentheses are the integrated intensity of CO(a) per gram of Ru loaded (arbitrary unit).

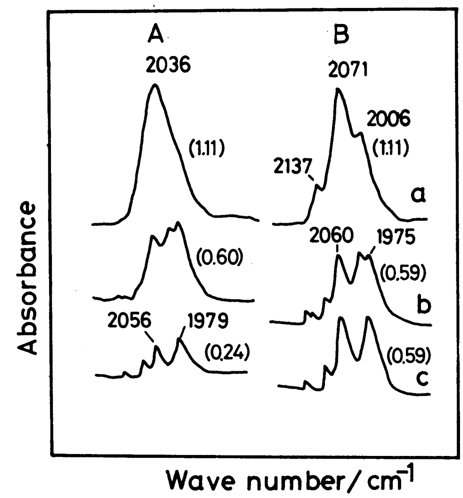

Fig. 7. Changes of infrared spectra of CO adsorbed on Ru/Al_2O_3 (A) by evacuation or hydrogenation: (A) 2.5 wt% (B) 0.9 wt%; (a) after evacuation at 25 °C, (b) after evacuation at 200 °C, (c) after the reaction with H_2 (100 mmHg) at 200 °C, for 1 h.

Figures in parentheses are the integrated intensity of CO(a) per gram of Ru loaded (arbitrary unit).

Infrared Spectra of CO Adsorbed on Ru/Al_2O_3. CO adsorbed is denoted as CO(a) hereafter. Figures 6 and 7 show infrared spectra of CO(a) on Ru/Al_2O_3 (B) and Ru/Al_2O_3 (A), respectively. Spectra a and b in these figures were recorded after evacuation at 25 and 200 °C, respectively. Spectra c were taken after the reaction of CO(a) with H_2 (100 mmHg) at 200 °C for 1 h. Over Ru/Al_2O_3 (B), three well resolved bands appeared at 2137—2141, 2073—2083, and 2013—2029 cm^{-1} after the evacuation at 25 °C (Fig. 6). Both the shape and position of the bands were almost independent of the loading amount of Ru. The evacuation at 200 °C caused complete elimination of the highest frequency band and a considerable decrease in the medium frequency band. The remaining CO(a) showed a paired band located at 2075—2087 and 2009—2021 cm^{-1}. As the dispersion increases, the relative intensity of the paired band increases (spectra b in Fig. 6). CO(a) on Ru/Al_2O_3 (A) gave a broad band, as shown in Fig. 7.

Figure 8 shows the relationship between the dispersion and the band intensity of the inactive CO(a). The relative amount of the inactive CO(a) significantly increased as the dispersion increased for each series of Ru/Al_2O_3. Infrared spectra of CO(a) taken under the reaction conditions are shown in Fig. 9. The spectra in the region of CO stretching were essentially unchanged during the reaction for 3 h. Bands attributable to CH_x stretching frequencies observed between 2800 and 3000 cm^{-1} continued to increase with the reaction time, in agreement with the result reported before.[11,13] Over 0.9% Ru/Al_2O_3 (A), two strong bands can be seen at 2056 and 1979 cm^{-1}, while broad bands appeared near 2033 cm^{-1} over 2.5% and 4% Ru/Al_2O_3 (A), and 2.5% Ru/Al_2O_3 (B). The relative amounts of CO(a) per gram of Ru during the reaction, which were estimated from the area of the bands, were fairly consistent with those obtained by chemisorption (CO/Ru in Table 1).

Discussion

Dispersion and CO Adsorption Data. Chemisorption data in Table 1 demonstrate that the dispersion of Ru/Al_2O_3 (A) is rather high, even at high loading levels, compared with that of Ru/Al_2O_3 (B). Kellner and Bell[4] observed that the dispersion of 1.3% Ru/Al_2O_3, which was prepared from $[Ru_3(CO)_{12}]$, decreased to 60% from 90% during a reaction cycle of CO hydrogenation. They attributed the decrease to the rapid growth of Ru particles, which was accelerated by the temperature rise due to the heat of reaction. However, in the present work the dispersion of 4% Ru/Al_2O_3 (A) decreased from 80% to only 74% after the use for reaction. So, the dispersion of the fresh catalysts may be used as "dispersion" during the reactions carried out in this work.

In chemisorption of CO, the CO/Ru ratio exceeded unity at low loading levels, in agreement with the results of Kobayashi and Shirasaki[18] and Dalla Betta.[19] This suggests that more than two molecules of CO are adsorbed on a single Ru atom, that is, multiple CO adsorption. One hydrogen atom may be considered to be adsorbed on the surface of one Ru atom at 1:1 stoichiometry, since it was reported that the particle size calculated from hydrogen adsorption agreed with that obtained from electron micrographs on Ru/Al_2O_3 and Ru/SiO_2.[16] Accordingly, the ratio in the uptake of CO to hydrogen atom (CO/H) gives the average number of CO molecules attached on each surface Ru atom. The CO/H ratio for Ru/Al_2O_3 (A) was less than 1.65, suggesting that the linear-type CO (Ru-CO) occupied a considerable part of the surface sites. The IR band at about 2036 cm^{-1} for 2.5% Ru/Al_2O_3 (A) (Fig. 7) is assigned to the linear-type CO on the basis of the previous studies.[13,14] As shown in Fig. 7, a considerable amount of linear-type CO is present on 2.5% Ru/Al_2O_3 (A).

The paired IR band observed on these Ru/Al_2O_3 catalysts was quite similar to that of the twin-type CO on Ru/Al_2O_3.[20] It is known that $[Rh_2(CO)_4Cl_2]$ and

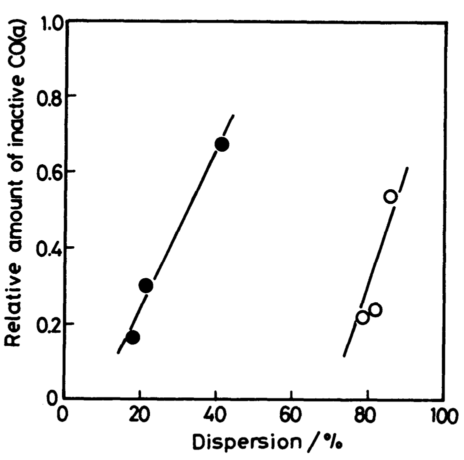

Fig. 8. Relationship between the relative amount of inactive CO(a) and the dispersion:
○: Ru/Al_2O_3 (A), ●: Ru/Al_2O_3 (B).
The ordinate shows the integrated intensity of bands normalized by that of bands obtained after evacuation at 25 °C.

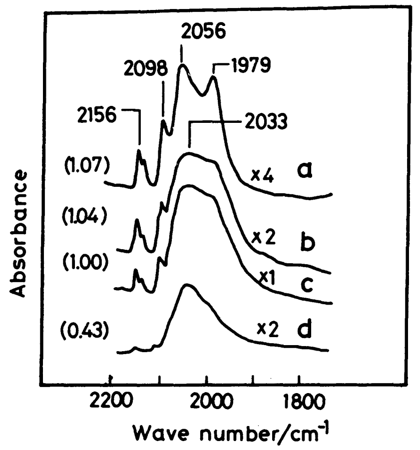

Fig. 9. Infrared spectra obtained under reaction conditions:
(a) 0.9% Ru/Al_2O_3 (A), (b) 2.5% Ru/Al_2O_3 (A), (c) 4% Ru/Al_2O_3 (A), (d) 2.5% Ru/Al_2O_3 (B).
Spectra were taken after 2 h under reaction at 200 °C (P_{H_2}=200 mmHg, P_{CO}=60 mmHg).
Figures in parentheses are the integrated intensity of CO(a) per gram of Ru loaded (arbitrary unit).

$[Ru(CO)_2X_n]$ (X=halogen)[21] shows a paired band associated with the symmetric and assymmetric vibration of the coordinated CO. Accordingly, the paired band observed on Ru/Al_2O_3 can be assigned to the twin-type CO, as reported by Kellner and Bell.[9] In the case of Ru/Al_2O_3 (B), the twin-type CO is the main species on the surface (Fig. 6). However, the CO/H values higher than 3 observed for 0.5% Ru/Al_2O_3 (B) seem to be unusual and the exact structure is not clear. The increase in the CO/H with the Ru dispersion suggests that adsorption sites available for the multiply bonded CO are edge or corner sites of Ru particles. The absence of twin-type CO on a single crystal surface of Ru[22,23] supports the assertion that the twin-type CO is formed on the edge or the corner sites of Ru particles.

Activity, Selectivity vs. *Dispersion.* Although low catalytic activity of low loading Ru/Al_2O_3 (A) is consistent with the result of Kellner and Bell,[4] the high activity of 4% Ru/Al_2O_3 (A) in the CO hydrogenation is a noticeable feature of Ru/Al_2O_3 (A) (Fig. 1). The change of TOF with the dispersion for the CO hydrogenation (Fig. 4) is not so simple as reported by King.[2] One possible reason for the two distinct correlations for Ru/Al_2O_3 (A) and Ru/Al_2O_3 (B) is the effect of the chloride ion remaining on Ru/Al_2O_3 (B) after reduction, but its effect is not known exactly. In any event, Fig. 4 suggests that the TOF for the CO hydrogenation cannot be determined only by the dispersion. Actually, Kikuchi *et al.* showed that the value of the TOF depended on the nature of the supports.[5] Moreover, the pre-oxidized 2.5% Ru/Al_2O_3 (A) showed a rather low TOF in spite of the low dispersion (Fig. 4).

In order to explain the change of the TOF, Kellner and Bell supposed that the electron density was reduced by the interaction with the support as the Ru particle size decreased, and that this led to the weakening of CO adsorption and the reduction of the ability to dissociate CO over highly dispersed catalysts.[4] Contrary to the idea of Kellner and Bell, CO was more strongly adsorbed as the Ru particle size decreases, as shown in Figs. 6 and 7. If the strongly bonded CO dissociates more easily, the TOF would increase with dispersion.

As shown in Figs. 6 and 7, the twin-type CO is more strongly held than the linear-type CO. Comparison of spectra b with c in Figs. 6 and 7 reveals the reactivity of CO(a) toward hydrogenation. Only a small decrease in the band intensity was observed for low loading catalysts after the reaction with H_2 (0.5% Ru/Al_2O_3 (B) and 0.9% Ru/Al_2O_3 (A)), indicating that the twin-type CO was almost inactive for the hydrogenation. It may be emphasized that the relative concentration of inactive twin-type CO increased with the dispersion over each series of Ru/Al_2O_3 (Fig. 8). If one compares these trends with the change of TOF (Fig. 4), it may be stated that the TOF is inversely correlated with the surface concentration of inactive twin-type CO and that the structure-sensitive behavior in the CO hydrogenation is explained by the poisoning effect of the inactive CO. That is, the TOF decreased with the dispersion, since the increasing portion of active sites is occupied by the inactive twin-type CO.

Since the linear-type CO readily reacted with H_2 compared with the twin-type CO (Fig. 7), weakly bonded linear-type CO is probably catalytically active for this reaction. Indeed, only a small amount of linear-type CO is present on the less active 0.9% Ru/Al_2O_3 (A), while other catalysts have a considerable amount of this species under the reaction conditions (Fig. 9). In contrast to the CO hydrogenation, the TOF for the hydrogenolysis of ethane changed little (Fig. 5). This may be explained by the absence of the poisoning materials in this reaction.

Another important feature of Ru/Al_2O_3 (A) is seen in the olefin/paraffin ratio in the product hydrocarbons. As shown in Fig. 2, the ratio in C_2, C_3, and C_4 hydrocarbons increases as the dispersion increases. If the olefin/paraffin ratio is determined by the relative rate of the two processes,[24] *i.e.*, β-elimination of hydrogen from and hydrogen addition to surface alkyl intermediates, the ratio will be controlled by whether the sites adjacent to the alkyl intermediates are empty or occupied by hydrogen atoms. In this case, the olefin/paraffin ratio depends on the ability of hydrogenation under the reaction conditions. It is known that CO(a) acts as a poison for the dissociative adsorption of H_2. Accordingly, the strength of CO(a) would affect the ability of hydrogenation. Since the strength of CO adsorption increased with the Ru dispersion (Figs. 6 and 7), the increase of the olefin/paraffin ratio can be explained in terms of the inhibition of hydrogen-activation by adsorbed CO.

The possibility of the chain growth is essentially independent of the dispersion as shown in Fig. 2, which is consistent with the data of King[2] and Bell *et al.*[4] for supported Ru catalysts. Although a drastic decline in chain growth for higher hydrocarbons was observed in the case of Ru/Y-zeolite,[25] this is probable due to the cage effect of the zeolite and not to the size effect of Ru particles.

The present work partially supported by a Grant-in-Aid for Scientific Research Nos. 56045031 and 57045025 from the Ministry of Education, Science and Culture.

References

1) M. A. Vannice, *J. Catal.*, **37**, 449 (1975).
2) D. L. King, *J. Catal.*, **51**, 386 (1978).
3) R. A. Dalla Betta, A. G. Piken, and M. Shelef, *J. Catal.*, **35**, 54 (1974).
4) C. S. Kellner and A. T. Bell, *J. Catal.*, **75**, 251 (1982).
5) E. Kikuchi, H. Nomura, and Y. Morita, Preprint of the 6th Japan-Soviet Catalysis Seminar, 1981, Osaka, p. 36.
6) T. Fukushima, T. Nobusawa, K. Fujimoto, and H. Tominaga, *Nippon Kagaku Kaishi*, **1982**, 177.
7) M. A. Vannice, *J. Catal.*, **40**, 129 (1975).
8) T. Okuhara, K. Kobayashi, T. Kimura, M. Misono, and Y. Yoneda, *J. Chem. Soc., Chem. Commun.*, **1981**, 1114.
9) C. S. Kellner and A. T. Bell, *J. Catal.*, **71**, 296 (1981).
10) T. Okuhara, T. Kimura, M. Misono, and Y. Yoneda, Preprint of the 6th Japan-Soviet Catalysis Seminar, 1981, Osaka, p. 28.
11) R. A. Dalla Betta and M. Shelef, *J. Catal.*, **48**, 111 (1977).

12) H. Yamasaki, Y. Kobori, S. Naito, T. Onishi, and K. Tamaru, *J. Chem. Soc., Faraday Trans. 1*, **77**, 2913 (1981).

13) D. L. King, *J. Catal.*, **61**, 77 (1980).

14) J. G. Ekerdt and A. T. Bell, *J. Catal.*, **58**, 170 (1979).

15) T. Kimura, T. Okuhara, M. Misono, and Y. Yoneda, *Nippon Kagaku Kaishi*, **1982**, 162.

16) R. A. Dalla Betta, *J. Catal.*, **34**, 57 (1974).

17) M. A. Vannice, *J. Catal.*, **37**, 462 (1975).

18) M. Kobayashi and T. Shirasaki, *J. Catal.*, **28**, 289 (1973).

19) R. A. Dalla Betta, *J. Phys. Chem.*, **79**, 2519 (1975).

20) D. J. C. Yates, L. L. Murrell, and E. B. Prestridge, *J. Catal.*, **57**, 41 (1979).

21) V. L. Kuznetsov and A. T. Bell, *J. Catal.*, **65**, 374 (1980).

22) M. Deeba and B. G. Gates, *J. Catal.*, **67**, 303 (1981).

23) R. A. Dalla Betta, A. G. Piken, and M. Shelef, *J. Catal.*, **35**, 54 (1974).

24) A. T. Bell, *Catal. Rev.*, **23**, 203 (1981).

25) H. H. Nijs, P. A. Jacobs, and J. B. Uytterhoeven, *J. Chem. Soc. Chem. Commun.*, **1979**, 1095.